New Phytologist

SHORT INTERNODES-like genes regulate shoot growth and xylem proliferation in *Populus*

Christine Zawaski[1], Mahita Kadmiel[2], Cathleen Ma[3], Ying Gai[4], Xiangning Jiang[4], Steve H. Strauss[3] and Victor B. Busov[1]

[1]School of Forest Research and Environmental Science, Michigan Technological University, 1400 Townsend Drive, Houghton, MI 49931, USA; [2]Department of Cell and Molecular Physiology, University of North Carolina, Chapel Hill, NC 27599, USA; [3]Department of Forest Ecosystems and Society, Oregon State University, Corvallis, OR 97331-5752, USA; [4]National Engineering Laboratory for Tree Breeding, The Tree and Ornamental Plant Breeding and Biotechnology Laboratory of Forestry Administration of China, College of Life Sciences and Biotechnology, Beijing Forestry University, Beijing 100083, China

Author for correspondence:
Victor B. Busov
Tel: +1 906 487 1728
Email: vbusov@mtu.edu

Received: *30 December 2010*
Accepted: *13 March 2011*

New Phytologist (2011) **191**: 678–691
doi: 10.1111/j.1469-8137.2011.03742.x

Key words: biomass, *Populus*, SHORT INTERNODES (SHI), wood formation, xylem.

Summary

- Genes controlling plant growth and form are of considerable interest, because they affect survival and productivity traits, and are largely unknown or poorly characterized. The *SHORT INTERNODES (SHI)* gene is one of a 10-member *SHI-RELATED SEQUENCE (SRS)* gene family in *Arabidopsis* that includes important developmental regulators.
- Using comparative sequence analysis of the *SRS* gene families in poplar and *Arabidopsis*, we identified two poplar proteins that are most similar to *SHI* and its closely related gene *STYLISH1 (STY1)*. The two poplar genes are very similar in sequence and expression and are therefore probably paralogs with redundant functions.
- RNAi suppression of the two *Populus* genes enhanced shoot and root growth, whereas the overexpression of *Arabidopsis SHI* in poplar reduced internode and petiole length. The suppression of the two genes increased fiber length and the proportion of xylem tissue, mainly through increased xylem cell proliferation. The transgenic modifications were also associated with significant changes in the concentrations of gibberellins and cytokinin.
- We conclude that *Populus SHI-RELATED SEQUENCE* (*SRS*) genes play an important role in the regulation of vegetative growth, including wood formation, and thus could be useful tools for the modification of biomass productivity, wood quality or plant form.

Introduction

The *SHORT INTERNODES* (*SHI*) gene is the founding member of a 10-member *SHI-RELATED SEQUENCE (SRS)* gene family in *Arabidopsis* (Fridborg *et al.*, 1999, 2001). Members of the *SRS* family include important developmental regulators, such as *LATERAL ROOT PRIMORDIA 1 (LPR1), STYLISH1 (STY1), STYLISH2 (STY2)* and *SRS7* (Fridborg *et al.*, 2001; Kuusk *et al.*, 2006; Kim *et al.*, 2010). The family displays high sequence divergence, except for two highly conserved regions: a RING-like zinc finger and an IGGH domain unique to SRS proteins (Fridborg *et al.*, 2001; Kuusk *et al.*, 2006). Similar RING-like zinc finger proteins have been implicated in transcriptional regulation and in the mediation of protein–protein interactions involved in the ubiquitination of targets for proteasomal degradation (Fridborg *et al.*, 2001). Despite the high sequence divergence amongst SRS genes, the analysis of double, triple, quadruple and quintuple loss-of-function mutants revealed high functional redundancy among the different family members (Kuusk *et al.*, 2006). *SHI* and the closely related *STY1* and *STY2* genes are thought to act synergistically to promote gynoecium, stamen and leaf development (Kuusk *et al.*, 2006). Recently, *SRS7* has been implicated in the regulation of tapetum dehiscence (Kim *et al.*, 2010). The overexpression

of *STY1*, *STY2* and *SRS7* has been shown to reduce stem elongation in a similar manner as that observed with *SHI* overexpression (Kuusk *et al.*, 2002; Kim *et al.*, 2010).

The mechanism of SRS action is not fully understood. Recently, STY1 has been shown to act as a transcription factor that activates auxin biosynthesis by direct binding to a specific *cis*-element in the promoter of the *YUCCA4* gene, which encodes a flavin monooxygenase – a rate-limiting enzyme in a tryptophan (Trp)-dependent auxin biosynthetic pathway (Sohlberg *et al.*, 2006; Eklund *et al.*, 2010). Inducible up-regulation of *STY1* led to increased auxin (indole acetic acid, IAA) concentrations (Sohlberg *et al.*, 2006), whereas ectopic expression of SHI increased the levels of bioactive gibberellins (GAs) (Fridborg *et al.*, 1999). Although some of these responses may result from complex feedback regulatory circuits, the data strongly point to important roles of SRS proteins in coordinating multiple hormonal pathways that modulate growth and developmental networks.

Modifications to plant stature and form, via native alleles or transgenic manipulations, can provide agronomic benefits to yield, stress tolerance and management. For instance, the 'green revolution' semi-dwarf varieties of cereal crops, such as wheat and rice, with defects in GA biosynthesis or signaling, have been widely used because they often show increased grain yield and harvest index, are resistant to lodging and respond better to nitrogen fertilization (Thomas & Sun, 2004). Such benefits were instrumental in averting the food shortages facing South-East Asia in the 1960s (Sasaki *et al.*, 2002). The effects of other genes that control plant stature, form and productivity, such as SRS genes, are poorly understood and may provide additional growth-related benefits for a variety of crop species.

Populus is both economically and ecologically important, and has emerged as the model species for the dissection of woody perennial biology (Wullschleger *et al.*, 2002; Busov *et al.*, 2005; Jansson & Douglas, 2007). With more than 30 species and a wide distribution throughout the Northern Hemisphere, *Populus* plays several important ecological roles, such as being a pioneer species in boreal and a dominant species in riparian forests (Braatne *et al.*, 1992). Economically, it is significant worldwide for its use in wood-based products (e.g. paper and timber) and, in North America, *Populus* is the primary short-rotation woody crop (Graham, 1994). Therefore, an understanding of the control of biomass productivity and tree architecture in *Populus* could provide a useful means for the modulation of production traits via genetic engineering or conventional plant breeding.

In this article, we demonstrate that, in *Populus*, two putative *SHI*-like sequences have redundant functions, and that transgenic manipulation of *SHI* activity provides useful modifications to tree growth, form and wood properties.

Materials and Methods

Sequence analysis

The *SRS* sequences used in the phylogenetic analysis were as follows: *SHI* (At5g66350.1), *AtSTY1* (At3g51060.1), *AtSTY2* (At4g36260.1), *AtLRP1* (At5g12330.1), *AtSRS3* (At2g21400.1), *AtSRS4* (At2g18120.1), *AtSRS5* (At1g 75520.1), *AtSRS6* (At3g54430.1), *AtSRS7* (At1g19790.1). *AtSRS8* (At5g12300) was excluded because it has been found previously to be a pseudogene (Kuusk *et al.*, 2006). We identified *Populus* orthologs of *SRS* genes via homology searches in version 2 of the *Populus trichocarpa (P. trichocarpa = Pt)* genome sequence (http://www.phytozome.net/) (Table 1). For consistency, the nomenclature of *Populus SRS* genes followed Kuusk *et al.* (2006). Whole protein sequences were used in the comparative sequence analyses. The sequences were aligned with ClustalW (http://www.ebi.ac.uk/Tools/clustalw2/index.html), and a phylogenetic tree was constructed with MEGA4 (http://megasoftware.net/mega4/mega.html) using the neighbor-joining method. Confidence was assessed by bootstrapping (1000 replications).

Table 1 Names and genome locations of the 10 poplar *SHI (SHORT INTERNODES)-RELATED SEQUENCE (SRS)* genes

Gene name	Gene identifier	Genome position
PtSRS1[1]	POPTR_0009s12450	scaffold_9: 10162482 – 10163346
PtSRS2	POPTR_0004s16770	scaffold_4: 17130963 – 17131880
PtRSR3/PtSHI2	POPTR_0005s12020	scaffold_5: 8799950 – 8801977
PtSRS4	POPTR_0002s03000	scaffold_2: 1860209 – 1861630
PtSRS5	POPTR_0005s25560	scaffold_5: 23795059 – 23796493
PtSRS6	POPTR_0001s28290	scaffold_1: 27068183 – 27069943
PtSRS7	POPTR_0009s07510	scaffold_9: 6989363 – 6991937
PtSRS8	POPTR_0003s19550	scaffold_3: 18247555 – 1824916
PtSRS9	POPTR_0001s06500	scaffold_1: 5008678 – 5011974
PtSRS10/PtSHI1	POPTR_0007s13610	scaffold_7: 13653593 – 13655374

[1]Used model eugene3.00090456 in comparative sequence analysis from version 1.1 as, in version 2, the predicted protein sequence is truncated.

Production of binary vector

For the generation of the RNAi construct (i.e. *PtSHI1_2*-RNAi), a 237-bp region of the *PtSHI2* sequence was PCR-amplified from poplar genomic DNA using the primers 5′-*GGGGACAAGTTTGTACAAAAAAGCAGGCT*-TGGCAACCAAGCAAAGAAAG-3′ and 5′-*GGGGACCA-CTTTGTACAAGAAAGCTGGGT*CGAGTGCAAGCAAG-AGAAG-3′, which contained attB1 and attB2 sites (italic) for GATEWAY BP cloning. The amplified sequence from *PtSHI2*, used in the RNAi construction, was chosen because of its high similarity to *PtSHI1* (92% nucleotide identity), with the intention of suppressing both genes, and thus the construct was denoted as *PtSHI1_2*-RNAi. The amplified fragment was cloned into the RNAi pHellsgate2 vector using the GATEWAY system following the manufacturer's instructions (Invitrogen, Carlsbad, CA, USA).

A cDNA clone of the *Arabidopsis SHI* gene was kindly provided by Dr Eva Sundberg (Swedish University of Agriculture Sciences, Uppsala, Sweden), and used in the generation of the overexpression construct (*35S::SHI*). The open reading frame was PCR-amplified using the following primers: forward, 5′-*GGATCC*ATGGCAGGATTTTTC TC-3′; reverse, 5′-*TCTAGA*TCAAGATCTTGAGTTGG AGA-3′; these contain *BamH1* and *Xba1* sites (italic). The amplified fragment (1008 bp) was inserted into the pART7 shuttle vector using the respective *BamH1* and *Xba1* sites, downstream of the CaMV35S (35S) promoter and upstream of the octopine synthase (OCS) terminator. The expression cassette was transferred into the pART27 binary vector using the *Not1* restriction site (Gleave, 1992). All constructs were sequence verified before transformation.

Agrobacterium-mediated transformation

The binary vectors were transformed into *Agrobacterium tumefaciens* via the freeze and thaw method (Holsters *et al.*, 1978). Strain C58 was used for the transformation of over-expression constructs, and AGL1 for the transformation of the RNAi vector. Positive colonies were PCR-verified for the presence of the vectors.

All transformation work was performed in a highly transformable *Populus tremula* × *P. alba* clone, INRA 717-IB4 (717), using a previously described protocol (Filichkin *et al.*, 2006). Twenty independent events were generated for each of the *PtSHI1_2*-RNAi and *35S::SHI* constructs. All transgenics used for subsequent analysis were first PCR-verified for the presence of the transgene. For the *35S::SHI* plants, we used the following primers: 5′-AGCAC GACACTCTGGTCTAC-3′ and 5′-TATTAGTTCGC CGCTCGGTG-3′. To safeguard against possible rearrangements because of the close proximity of repeats in the RNAi vector, we validated the integrity of both the promoter and terminator junctions using two primer sets: (1) *35S* forward, 5-AGCACGACACTCTGGTCTAC-3′ and *PtSHI1_2*-RNAi reverse, 5′-AGTCGAGTGCAAGCAAG-AGAAG-3′; and (2) *PtSHI1_2*-RNAi forward, 5′-AGTCG-AGTGCAAGCAAGAGAAG-3′ and *OCS* reverse, 5′-ATT-AGTTCGCCGCTCGGTG-3′.

Reverse transcription-polymerase chain reaction (RT-PCR) and quantitative real-time RT-PCR analyses

Total RNA was isolated using the RNeasy Plant Mini Kit (Qiagen, Valencia, CA, USA) with on-column genomic DNA digestion using RNase-free DNase (Qiagen). cDNA was synthesized from 2 μg of DNaseI-treated total RNA using Superscript III reverse transcriptase (RT; Invitrogen) and oligo-dT primer.

Quantitative real-time RT-PCR was used to measure relative expression differences in *SHI*-modified transgenic plants. Real-time PCR was performed using Maxima SYBR Green QPCR Master Mix (Fermentas, Glen Burnie, MD, USA) and an ABI StepOnePlus System (ABI, Foster City, CA, USA). The primers used in the expression analyses are shown in Supporting Information Table S1. Each PCR was run under the following conditions: one cycle at 95°C for 10 min; 40 cycles at 95°C for 15 s, 60°C for 30 s and 72°C for 30 s; followed by a thermal denaturation step to derive dissociation curves. At least three biological replications were used in each experiment. Expression was calculated using the $2^{-\Delta\Delta Ct}$ method (Livak & Schmittgen, 2001). The expression of the ubiquitin-like gene was used as a loading control (Table S1).

The expression of *PtaSHI1* and *PtaSHI2* in different organs and genetic backgrounds was studied using semi-quantitative RT-PCR. We used a variable number of cycles to determine the linear range of amplification for each gene, including the loading control genes. Real-time PCR using Brilliant SYBR Green QPCR Master Mix (Stratagene, La Jolla, CA, USA) and MX3000P (Stratagene) was used to validate the linear range of amplification. Primers for the amplification of each gene are given in Table S1. The optimized PCR conditions were as follows: *PtaSHI1*: 32 cycles at 95°C for 30 s, 60°C for 30 s and 72°C for 60 s; *PtaSHI2*: 32 cycles at 95°C for 30 s, 58°C for 30 s and 72°C for 60 s; *Ubiquitin*: 29 cycles at 95°C for 30 s, 55°C for 30 s and 72°C for 30 s. All PCRs were run on ethidium bromide-stained 1.5% agarose gels. Digital images and the quantification of ethidium bromide fluorescence were made using the GelDoc-It Imaging System and VisionWorksLS software, respectively (UVP Ltd, Cambridge, UK). At least three biological replications and two technical replications were used in each experiment.

Phenotypic characterization and measurements

All transgenics were first propagated *in vitro* on hormone-free medium. After 1 month of *in vitro* growth, plants were

transferred to a glasshouse and grown under standard irrigation, fertilization and pest control. Plants were measured and harvested at 60 d for all 35S::*SHI* plants and at 70 d for all *PtSHI1_2*-RNAi plants. Tissues for dry biomass estimation were dehydrated at 70°C until they reached a constant weight.

In vitro root data were obtained from digital photographs taken from the bottom of Magenta boxes, and subsequent measurements were made with ImageJ 1.38v software (National Institutes of Health, Bethesda, MD, USA).

Microscopy and fiber length measurement

Stem segments from *PtSHI1_2-RNAi* transgenic event R1 with three ramets were sampled at the 20th internode, and immediately fixed in formalin–acetic acid–alcohol and processed using Shandon Excelior and Histocentre 2 (Thermo Scientific Co., Waltham, MA, USA). Five-micrometer-thick sections were stained with hematoxylin and eosin. For fiber length analysis, a modified version of Franklin's maceration method was used (Franklin, 1945). Stem segments from the 20th internode were incubated at 60°C for 24 h in equal volumes of glacial acetic acid and hydrogen peroxide, followed by washing with distilled water. A small amount of the resulting pulp was stained with safranin O. Images of stem sections and fibers were captured using a Leitz Wetzlar fluorescent microscope (Ernst Leitz, Wetzlar, Germany) with a SPOT Insight QC camera and advanced SPOT software (Diagnostic Instruments, Sterling Heights, MI, USA). Measurements were made from images in ImageJ 1.38v software (National Institutes of Health).

Hormone measurements

Expanding leaves were harvested from 1-yr-old glasshouse-grown transgenic and wild-type (WT) plants, each line represented by three independent ramets. The samples were quickly fresh weighed, flash frozen and powdered in liquid nitrogen, and subsequently lyophilized. Samples were extracted in 80% methanol with the internal standards $[^2H_2]$-GA_8, $[^2H_2]$-GA_1, $[^2H_2]$-GA_{20}, $[^2H_2]$-GA_{19}, $[^2H_2]$-GA_{34}, $[^2H_2]$-GA_4, $[^2H_2]$-GA_{53}, $[^2H_2]$-GA_9, $[^2H_2]$-GA_{12} and $[^{13}C_6]$-IAA overnight, and reduced to aqueous phase by vacuum. The aqueous phase was adjusted to pH 3.0 and partitioned with ethyl acetate; the organic phase was then repartitioned with K–Pi buffer (pH 8.5), and the aqueous phase was adjusted to pH 3.0 and partitioned again with ethyl acetate. Further purification was performed on C_{18} Sep-Pak and MCX SPE columns (Oasis; Waters Ltd, Milford, MA, USA). The eluate was dried, redissolved in HPLC (high-performance liquid chromatography) initial solution, filtered through a 0.22-μm filter and analyzed with an LC/MS (liquid chromatography/mass spectrometry) system (LCQ Deca MAX, HPLC-ESI-MS; Thermo-Finnigan, San Jose, CA, USA). MS–MS data were then analyzed using the software Xcalibur 2.1 (Thermo-Finnigan), and quantified by reference to ratios of specific ions of phytohormones in natural samples over those of internal standards using equations for isotope dilution analysis. Cytokinins were measured essentially as described previously (Chen *et al.*, 2010).

Statistical analysis

All statistically analyzed experiments were carried out as completely randomized designs, and hypothesis tests were conducted using a significance level of 0.05. Data were represented as event means of at least four ramets for *PtSHI1_2*-RNAi transgenics and at least seven ramets for *35S::SHI* transgenics. WT untransformed 717 plants were used as controls. Analysis of variance (ANOVA) was used to test for significant differences in event means. When significant differences were present, Dunnett's test was used to make multiple comparisons with WT, and Tukey's honestly significant difference (HSD) test was used to make all pairwise comparisons. Regression analysis was used to determine the relationship between transgene expression and measured traits. Standard error bars were based on at least three biological replications. Statistical analysis was performed with SigmaStat (Systat Software Inc., San Jose, CA, USA).

Results

Identification and expression of *SHI* orthologs in *Populus*

Previously, nine *SRS* genes were identified by searching an earlier draft of the *Populus* genome sequence (Kuusk *et al.*, 2006). We isolated an additional gene by searching the most recent draft of the poplar genome sequence, which was not reported previously (Table 1). For consistency with previous work, the newly discovered member was named *PtSRS10*. Despite the recent salicoid duplication in *Populus*, the *SHI* gene family has not expanded relative to *Arabidopsis*, and thus several of the duplicated gene pairs have probably not been retained. These findings are similar to previous work, suggesting that *Populus* has a similar number of zinc finger, RING-type proteins as *Arabidopsis* (Yang *et al.*, 2008).

Using the poplar and *Arabidopsis* sequences, we performed comparative sequence analysis (Fig. 1a). The topology of the current tree is very similar to that published previously based on the nine poplar SRS protein sequences, although some differences do occur, probably as a result of the different genome drafts used to infer the protein sequences (Kuusk *et al.*, 2006). The family is clearly divided into two separate lineages with one containing LATERAL ROOT PRIMORDIA1 (LRP1) and AtSRS6 from *Arabidopsis* together with four poplar proteins: PtSRS6 and

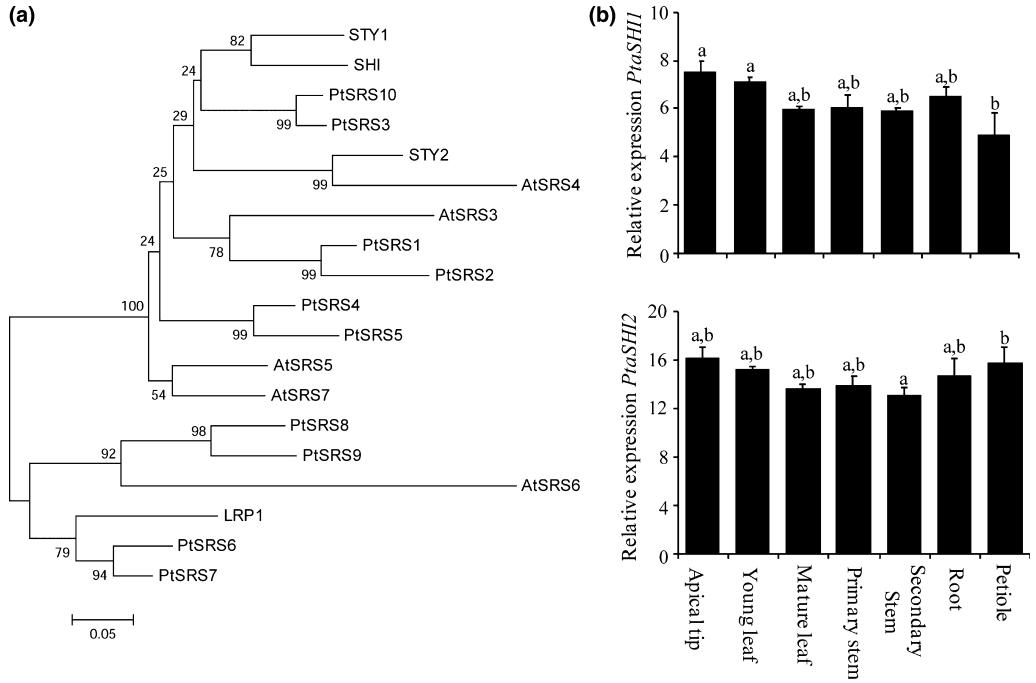

Fig. 1 Phylogenetic relationship between *Arabidopsis* and *Populus* SHI (SHORT INTERNODES)-RELATED SEQUENCES proteins (a) and the expression of two *Populus SHI* orthologs in various wild-type (WT) tissues (b). In (a), sequences were aligned with ClustalW (http://www.ebi.ac.uk/Tools/clustalw2/index.html), and the phylogenetic tree was generated using MEGA4 (http://megasoftware.net/mega.html). Numbers at the branch points represent bootstrap support values. A full list of sequences used can be found in the Materials and Methods section and Table 1. In (b), reverse transcription-polymerase chain reaction (RT-PCR) was performed on total RNA extracted from different tissues collected from three independent biological repetitions of 3-month-old WT 717 plants. Bars represent the mean ± SE of *PtaSHI* and *PtaSHI2* expression normalized to *Ubiquitin*. 'Primary' refers to stems undergoing primary growth at the top of the plant, and 'Secondary' refers to stems undergoing secondary (woody) growth at the bottom of the plant. Different letters denote significant differences between tissues as determined by ANOVA followed by Tukey's *post-hoc* test ($P < 0.05$).

PtSRS7 more similar to LRP1, and PtSRS8 and PtSRS9 closer to AtSRS6. The other larger group was more difficult to resolve with respect to sequence similarity as most branches showed very weak bootstrap support between different phyletic clades. Nevertheless, some proteins, such as PtSRS4 and PtSRS5, formed an isolated lineage with high (99%) support. PtSRS1 and PtSRS2 clustered with AtSRS3. PtSRS3 and PtSRS10 were most closely related to the larger group of four *Arabidopsis* proteins including SHI, STY1, STY2 and AtSRS4. At least three of these proteins (SHI, STY1 and STY2) appear to be fully or partially redundant in function in *Arabidopsis* (Kuusk *et al.*, 2006). Both PtSRS3 and PtSRS10 showed highest sequence similarity to SHI and STY1 (Table 2). We therefore putatively named PtSRS10 as PtSHI1 and PtSRS3 as PtSHI2. We focused our further analysis on these two genes.

PtSHI1 and PtSHI2 sequences are highly similar (86% sequence identity), and we hypothesized that they may be functionally redundant. To gain further insight into the putative functional redundancy between *PtSHI1* and *PtSHI2*, we studied their expression in WT plants (i.e. *P. tremula* × P. alba, *PtaSHI1* and *PtaSHI2* expression) in different tissues and developmental stages. We found *PtaSHI1* and *PtaSHI2* to be expressed in all tissues tested (Fig. 1b). Both genes also showed similar expression patterns with slightly higher expression levels in shoot apices, young leaves and roots. However, the expression differences among different tissues were very small and not statistically significant.

Because ectopic expression of *SHI* in *Arabidopsis* interferes with GA signaling (Fridborg *et al.*, 1999), we tested whether the expression of the two *Populus SHI*-like genes was changed in transgenic poplar that had altered GA metabolism and signaling. Transgenic plants were available in our laboratory from earlier studies that had the same poplar genotype (717-1B4) as used in the current study (Busov *et al.*, 2003, 2006; Gou *et al.*, 2010). Indeed, both genes were found to be up-regulated in transgenic *Populus* overexpressing DELLA-less versions of *GAI* (*gai*) and *RGL1* (*rgl1*), and *GA 2-oxidase* (*PcGA2ox*) (Fig. 2).

RNAi-induced suppression of *PtaSHI* genes is associated with increased vegetative growth

The close sequence similarity and expression profiles suggested that the two *Populus SHI*-like genes may be functionally redundant. Therefore, we targeted both genes for RNAi suppression using a region of high sequence similarity. We recovered 20 independent events carrying the

Table 2 Protein similarity and identity matrix between *Arabidopsis* and poplar SHI (SHORT INTERNODES)-RELATED SEQUENCE (SRS) proteins generated by MAGAT and BLOSUM62

		Identity																			
	Similarity	1. SHI	2. STY1	3. STY2	4. AtSRS3	5. AtSRS4	6. AtSRS5	7. AtSRS6	8. AtSRS7	9. LRP1	10. PtSRS1	11. PtSRS2	12. PtSRS3	13. PtSRS4	14. PtSRS5	15. PtSRS6	16. PtSRS7	17. PtSRS8	18. PtSRS9	19. PtSRS10
1. SHI		**61.3**	42.6	26.9	34.1	37.5	20.2	42.3	34.6	32.9	34.0	**53.9**	45.0	42.7	30.6	31.2	30.7	30.3	**53.4**	
2. STY1	**71.6**		43.7	23.5	32.6	38.5	18.1	38.7	29.8	33.5	32.8	**55.7**	44.3	42.4	31.3	33.1	27.5	26.6	**57.5**	
3. STY2	59.5	57.8		26.7	46.3	35.2	22.5	34.6	31.2	30.1	30.3	40.9	37.7	35.8	33.1	34.0	30.7	30.6	43.1	
4. AtSRS3	35.6	32.4	35.1		28.5	24.8	25.8	27.0	22.3	43.3	41.8	25.6	27.4	27.9	21.5	20.8	22.8	24.7	26.1	
5. AtSRS4	44.7	41.6	53.7	41.4		31.3	25.1	28.4	29.2	30.9	28.7	33.3	31.4	31.7	26.3	25.6	28.0	29.2	35.4	
6. AtSRS5	58.1	54.3	52.6	32.9	41.0		22.3	63.0	29.1	31.4	29.9	44.4	50.3	45.9	31.5	31.1	30.1	29.2	45.8	
7. AtSRS6	31.1	27.3	33.9	48.6	43.2	31.8		23.1	27.4	22.8	20.6	20.9	20.8	20.5	23.2	23.2	31.4	31.9	22.7	
8. AtSRS7	57.1	53.5	53.6	33.3	39.4	75.4	32.5		29.9	28.7	27.5	44.0	47.6	44.4	30.4	29.6	29.7	28.2	44.9	
9. LRP1	51.1	43.0	50.3	32.8	39.1	43.9	38.1	41.2		26.8	23.6	29.2	30.5	30.8	50.7	52.9	36.6	37.0	29.1	
10. PtSRS1	41.1	41.6	38.8	59.0	46.4	38.7	44.4	39.1	35.3		76.3	37.8	38.9	39.8	24.3	24.8	26.0	27.2	37.4	
11. PtSRS2	43.2	43.2	39.1	54.4	45.9	38.7	42.4	39.1	35.6	80.2		36.6	38.2	35.8	24.7	25.3	25.7	26.8	37.4	
12. PtSRS3	**68.3**	**68.6**	61.0	33.7	41.3	61.6	32.6	63.2	44.2	44.5	43.6		54.7	48.4	30.4	30.9	28.8	27.0	85.9	
13. PtSRS4	61.9	59.2	51.9	35.2	43.3	65.6	31.5	60.6	45.5	45.2	46.4	67.4		80.2	30.0	30.1	28.9	28.0	55.1	
14. PtSRS5	58.0	55.1	51.9	37.1	46.6	58.1	31.3	57.7	45.6	47.6	46.3	61.9	82.9		29.5	28.7	25.6	25.9	50.4	
15. PtSRS6	47.0	46.8	48.7	29.7	34.6	47.9	33.4	45.9	66.6	32.6	34.6	46.5	43.3	41.4		85.4	36.8	35.6	31.0	
16. PtSRS7	45.8	47.3	47.8	29.8	36.8	47.8	34.0	44.9	67.1	33.7	34.8	48.6	43.0	42.4	91.9		38.9	36.1	29.8	
17. PtSRS8	47.1	41.4	46.6	35.0	44.4	43.6	44.4	42.6	52.8	38.8	39.5	43.9	45.2	45.2	51.3	50.6		79.7	29.3	
18. PtSRS9	44.4	38.1	46.6	34.2	43.1	39.6	43.1	39.1	52.5	37.0	36.7	42.7	40.2	43.5	49.3	50.0	85.7		27.1	
19. PtSRS10	**68.9**	**69.2**	64.7	33.7	44.1	57.8	34.0	60.3	47.1	45.0	46.5	89.5	67.8	61.4	47.3	47.2	45.6	42.2		

Poplar proteins start with the letters 'Pt'. Bold cells indicate highest similarity and identity to SHI and STYLISH1 (STY1).

Fig. 2 *PtaSHI1* and *PtaSHI2* expression is elevated in gibberellin (GA)-deficient (*35S::PcGA2ox1*) and GA-insensitive (*35S::rgl1* and *35S::gai*) *Populus* transgenics. Reverse transcription-polymerase chain reaction (RT-PCR) expression analysis (see the Materials and Methods section for details) was performed on total RNA from leaf samples collected in glasshouse (a) or field-grown (b) transgenic (open bars) and wild-type (WT; closed bars) plants. Bars represent event mean ± SE expression normalized to *Ubiquitin*. In (a), '1' and '2' after the transgenic type name indicate a relative reduction in stature, with 1 being taller and 2 shorter. In (b), the number in parentheses after the transgenic type name indicates the height (cm) of plants in the field. Asterisks denote significant differences between transgenic and WT events as determined by ANOVA followed by Dunnett's *post-hoc* test ($P < 0.05$).

construct and screened for the effect on the expression of the two endogenes using gene-specific primers. We found two events (R1 and R12) with strong and highly significant suppression of both genes (< 30% of the WT expression level; Fig. 3). Therefore, all subsequent experiments included these events.

To evaluate the effects of the RNAi modification on growth and development, we grew multiple clonally propagated ramets of the selected transgenic events under glasshouse conditions (Fig. 4a). The RNAi transgenic plants showed significant increases in several of the measured growth traits, including height, diameter, and leaf and petiole length (Fig. 4b–e).

To verify that the observed changes did not result from transgene-imparted suppression in other SRS members, we studied the expression of the four most closely related members from the subgroup in the R12 event that had the most dramatic suppression of both *PtSHI1* and *PtSHI2*. The subgroup members studied were *PtSRS*1, *PtSRS2*, *PtSRS4* and *PtSRS5* (Fig. 1, Table 2). We could not detect the expression of *PtSRS1* and *PtSRS2* in either the WT or transgenic plants, despite testing several primers and conditions. We

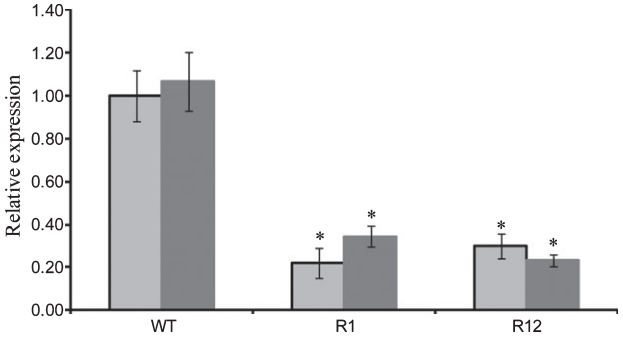

Fig. 3 Suppression of *PtaSHI1* and *PtaSHI2* in *PtSHI1_2*-RNAi transgenics. Bars represent event mean ± SE normalized to *Ubiquitin*. Quantitative real-time reverse transcription-polymerase chain reaction (RT-PCR) expression analysis (see the Materials and Methods section for details) was performed on total RNA extracted from leaves and stems of four ramets per transgenic event and four wild-type (WT) plants. *PtaSHI1* (light gray bars) and *PtaSHI2* (dark gray bars). Significance was determined by *t*-test (*, $P < 0.05$).

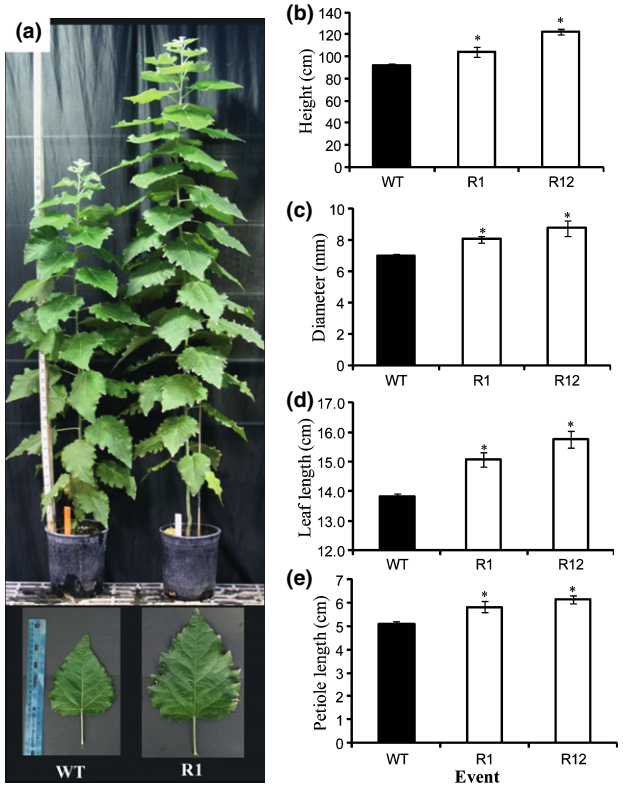

Fig. 4 Phenotypic changes in RNAi transgenics with severe suppression of *PtaSHI1* and *PtaSHI2*. Images were obtained from 60-d-old, glasshouse-grown, wild-type (WT) (left) and transgenic (right) plants (a). Bars represent event mean ± SE of nine ramets per transgenic event (open bars) and nine WT (closed bars) plants (b–e). Leaf and petiole measurements were performed at leaf plastochron index (LPI) 30. Asterisks denote significant differences between transgenic and WT events as determined by ANOVA followed by Dunnett's *post-hoc* test ($P < 0.05$).

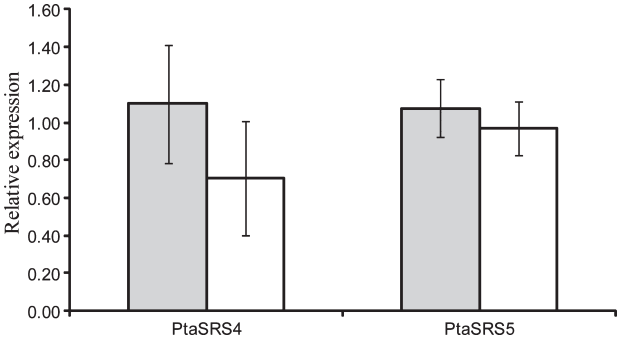

Fig. 5 Expression of *PtaSRS4* and *PtaSRS5* in RNAi transgenics. Bars represent event mean ± SE of three biological replications. *PtaSRS4* and *PtaSRS5* expression was normalized to *Ubiquitin* in RNAi line R12. Differences between R12 (open bars) and wild-type (WT) (closed bars) plants were not significant (*t*-test, $P < 0.05$).

were also unable to find any expressed sequence tags (ESTs) corresponding to these genes in the publicly available databases. Thus, they are either pseudogenes or expressed at very low levels and/or in a very specific manner. As such, the suppression of these two genes is unlikely to contribute to the observed phenotypic changes. By contrast, we were able to detect robust expression from both *PtSRS4* and *PtSRS5* (Fig. 5). Although a slight decrease in transcript abundance was obvious in both genes, and particularly in *PtSRS4*, the differences were not significant (Fig. 5).

PtaSHI gene suppression affects xylem cell proliferation and elongation

We investigated whether the increased diameter growth observed in the RNAi transgenics was accompanied by changes in wood structure and anatomy (Fig. 6a,b). We found that the increased diameter growth was primarily caused by an increased proportion of xylem (Fig. 6c); none of the other woody tissues measured were significantly different from those of WT plants (Fig. 6d,e). Likewise, there was a significant increase in xylem fiber length in the RNAi transgenics compared with WT (Fig. 6g). Because the increased proportion of xylem could result from an increase in cell number or cell size, we measured the radial cell size in a number of cross-sections at the same location. No significant changes in radial cell size for xylem fibers or vessel elements were detected (Fig. 6h,i), which suggests that the increased proportion of xylem is probably a result of increased xylem cell proliferation, not increased cell size.

SHI overexpression affects *Populus* leaf and root development

To better understand the conservation of SHI function between *Populus* and *Arabidopsis,* we overexpressed the *Arabidopsis SHI* gene in *Populus* using the *35S* promoter. Nine events were randomly selected from the population

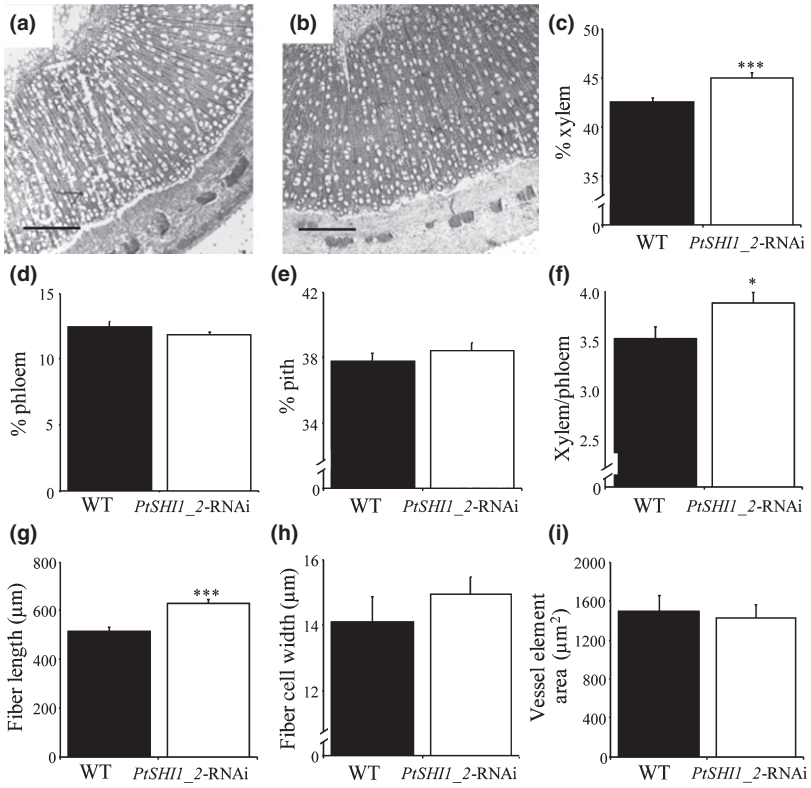

Fig. 6 RNAi transgenics are affected in secondary xylem development. Transverse stem sections and measurements were taken from the 20th internode of wild-type (WT; a, black bars) and *PtSHI1_2*-RNAi (b, white bars) stems. In (c–i), bars represent mean ± SE derived from the two *PtSHI1_2*-RNAi events, each with three ramets, and three WT plants. The xylem (c), phloem (d) and pith (e) are represented as a proportion of the total stem width. Fiber length was measured on macerated pulp from stem segments (at the 20th internode) on at least 60 fibers per ramet. Significance was determined by *t*-test (*, $P < 0.05$; **, $P < 0.01$; ***, $P < 0.001$). Bar, 0.5 mm.

of 20 for in-depth characterization. Expression analysis showed that overexpression of the *SHI* transgene indeed occurred in the selected events (Fig. 7a). *In vitro*, the *35S::SHI Populus* plants did not show dramatic changes in their aerial development (Fig. 7b). The effect of overexpression on height growth was minimal and not significantly different from WT plants (data not shown).

However, under *in vitro* conditions, the *35S::SHI* transgenics displayed significantly altered root development. Despite similar timing of root initiation, primary and lateral roots appeared longer and thicker in transgenics when compared with WT (Fig. 8a,b). To quantify these differences, we measured root development in three events with different transgene expression levels; events 1 and 2 had a high level of overexpression, whereas, for event 7, overexpression was moderate (Fig. 7a). We found that overexpression of *SHI* strongly affected lateral root development. Lateral root length was significantly increased, whereas density was significantly decreased, compared with WT roots (Fig. 8f,g). Although primary root length was greater in all transgenic events than in WT plants, the differences were not statistically significant (Fig. 8c,d).

Dose-dependent effects of *SHI* on growth in the glasshouse

Under glasshouse conditions, the internode length was more severely affected than the height (Fig. 9a–c). The majority of transgenic events showed significant reductions in internode length (Fig. 9c), whereas height was only significantly decreased in the two events with the highest transgene expression (Figs 7a, 9b). Lines with significant reductions in height were accompanied by significant decreases in internode length (Fig. 9c). Internode length was negatively correlated with internode number among the different transgenic events ($R^2 = 0.810$, $P < 0.004$).

One of the most striking effects of *SHI* overexpression was a large reduction in petiole length (Fig. 10a,b,d). The reductions in petiole length in the transgenic plants gave rise to a compact appearance, with leaves almost covering the whole stem (Fig. 9a). All transgenic leaves had a slight curvature at the edges of the leaf lamina (Fig. 10c).

Because of the almost continuous gradient of *SHI* expression levels in the different independent transgenic events (Fig. 7a), we studied whether the expression levels correlated with the severity of the observed phenotypic responses. Indeed, we found a significant linear relationship between the level of *SHI* and several of the measured traits (Fig. 11a–f).

Biomass allocation changes in RNAi and *SHI*-overexpressing plants

We calculated the biomass proportion as a ratio to that in WT planted at the corresponding times to compare *35S::SHI* and RNAi over different experiments (Table 3).

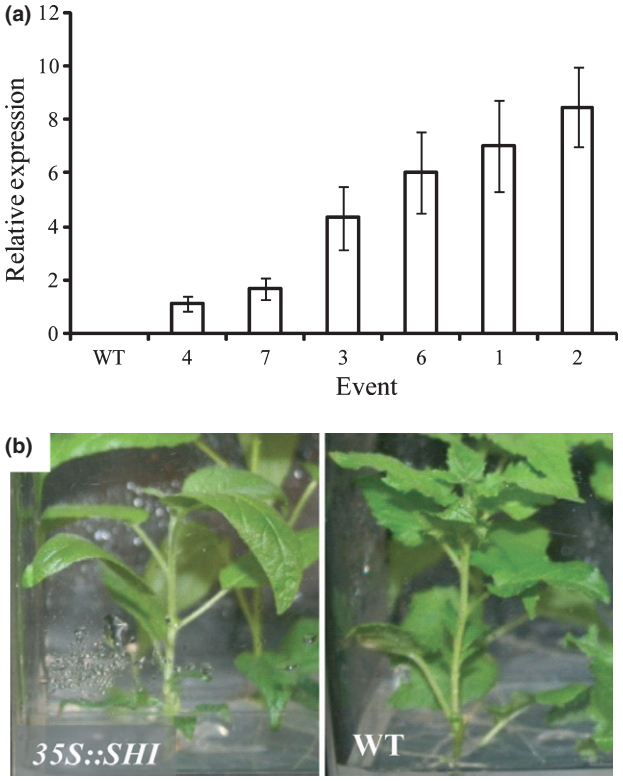

Fig. 7 Expression of *SHI* (*SHORT INTERNODES*) (a) and *in vitro* appearance (b) of *35S::SHI Populus* transgenics. Bars represent event mean ± SE of *SHI* expression normalized to *Ubiquitin*. Quantitative real-time reverse transcription-polymerase chain reaction (RT-PCR) was performed using total RNA pooled from leaves of seven ramets per transgenic event and 10 wild-type (WT) plants.

Consistent with our previous measurements, we observed a general increase in both aerial and root biomass for RNAi transgenics and a decrease for *SHI*-overexpressing transgenics.

Hormone changes in transgenic plants

Previously, it has been shown that ectopic expression of *SHI* results in changes in GA concentrations (Fridborg *et al.*, 1999), whereas the closely related STY1 activates auxin biosynthesis (Sohlberg *et al.*, 2006; Eklund *et al.*, 2010). We therefore studied GA and auxin concentrations in transgenic plants. Overexpression of *SHI* in *Populus* led to changes primarily in the early 13-hydroxylation pathway. Significant increases in bioactive GA1 and decreases in its precursors, GA_{20} and GA_{53}, as well as its inactive form, GA_8, were found (Table 4). By contrast, the RNAi transgenics showed changes in GAs derived from the 3-hydroxylation pathway, including decreases in the levels of GA_4 and its precursor GA_9 (Table 4). No significant changes were detected with respect to IAA concentrations (Fig. 12). Nevertheless, the *SHI*-overexpressing transgenics showed higher GA_1 concentrations relative to nontransgenic control plants and RNAi transgenics (Table 4). We also measured the concentrations of several cytokinins in transgenic plants (Table 4). Highly significant changes were measured for two cytokinins. The N^6-isopentenyladenine (IP) concentration was significantly lower in RNAi transgenics, whereas the N^6-isopentenyladenosine (IPR) level was significantly higher in *35S::SHI* transgenics.

Discussion

Sequence orthology and functional inferences of SRS proteins

The *SRS* gene family encodes proteins defined by a conserved RING finger-like zinc finger motif at the N-terminus and an IGGH domain at the C-terminus of the protein (Fridborg *et al.*, 1999; Kuusk *et al.*, 2006). Previously, nine poplar *SRS* sequences have been found by searches in an earlier draft of the poplar genome sequence (Kuusk *et al.*, 2006). In this article, we report an additional poplar member which was isolated from a search of the more advanced version 2 of the polar genome. Comparative analysis of *Arabidopsis* and poplar sequences indicates that the family has not expanded in *Populus* despite the recent genome-wide duplication in the salicoid lineage, and thus it is likely that most of the duplicated gene pairs were not retained. Nevertheless, high sequence conservation of several proteins, including the two genes under study, suggests that there are close paralogous relationships within the poplar gene family.

Low sequence conservation outside of the two conserved domains has impeded inferences with regard to the functional relationships between proteins (Kuusk *et al.*, 2006). For example, the family is clearly divided into two groups. A prominent member of the smaller group, LRP1 (see Fig. 1a), has been implicated in the regulation of lateral root primordia (Smith & Fedoroff, 1995). STY1 is a member of the other group, and loss-of-function mutation causes various defects in gynoecium development (Kuusk *et al.*, 2002; Sohlberg *et al.*, 2006). However, in double *sty1 lrp1* mutant plants, the lesion in LRP1 enhances the effects of the *sty1* loss-of-function mutation, suggesting at least partial redundancy between these two divergent proteins (Kuusk *et al.*, 2006). Likewise, we found it difficult to establish direct orthology between *Populus* genes and their *Arabidopsis* counterparts. Because we were interested in the *Populus SHI* gene, we identified two related sequences (i.e. *SHI*-like genes) that appeared to show highest similarity to *Arabidopsis SHI* and its closely related sequence STY1 (Fig. 1a). Because of the ambiguity of functional inferences based solely on sequence rather than functional characterization, we cannot unequivocally identify the *SHI* ortholog(s) in *Populus*. Difficulties in establishing sequence-

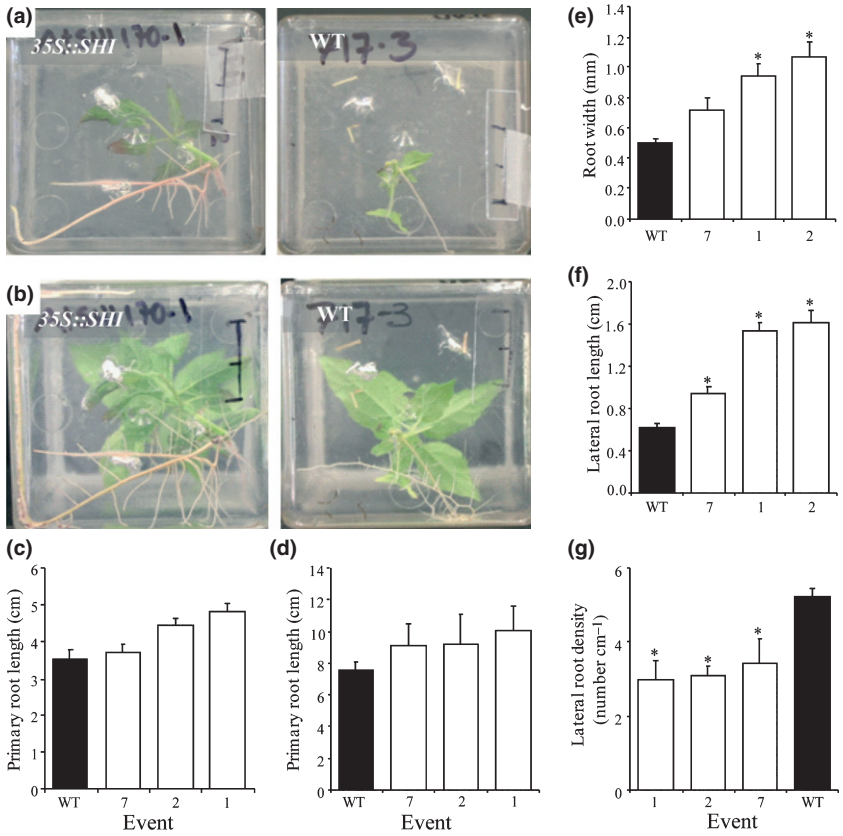

Fig. 8 Overexpression of *SHI* (*SHORT INTERNODES*) in *Populus* alters *in vitro* root development. Images illustrate differences in roots of transgenic and wild-type (WT) plants at 2 wk (a) and 4 wk (b) after root initiation. Bars represent event mean ± SE for 10 ramets. Primary root length was measured at 2 wk (c) and 4 wk (d) after root initiation. Measurements of root width, lateral root length and lateral root density were obtained at 4 wk after root initiation. Root width was measured 2 cm from the root–shoot junction (e). Asterisks denote significant differences between transgenic and WT events as determined by ANOVA followed by Dunnett's *post-hoc* test ($P < 0.05$).

based orthology, particularly in poorly conserved and rapidly evolving regulatory genes, are a major challenge for comparative and translational genomics, and underscore the importance of dissecting gene function.

Conservation of SHI function across distant lineages

To test whether SHI function is conserved across distant plant taxonomic lineages, we ectopically expressed *SHI* in transgenic *Populus* and studied whether the readily identifiable dwarf phenotype of *SHI*-overexpressing plants would be produced in transgenic *Populus*. We found that the overexpression of *Arabidopsis SHI* in *Populus* conferred a very mild dwarf phenotype in events with high levels of *SHI* overexpression (Fig. 9). The *SHI*-overexpressing *Populus* transgenics showed only 3% reduction in height relative to WT. The lack of a dwarf phenotype contrasts with the severe dwarfism seen from the ectopic expression of *SHI* in *Arabidopsis* (Fridborg *et al.*, 1999). Despite the mild effect on height in *Populus*, the average petiole length was severely reduced; it was 40% of that in WT (Fig. 10). This effect was not observed in *Arabidopsis* overexpressing the same gene (Fridborg *et al.*, 1999). However, the overexpression of *SHI* in *Populus* and *Arabidopsis* transgenics was comparable in that it caused a severe reduction in internode length (Fig. 9a,c). This is a common response to reductions in GA levels or sensitivity (Fleet & Sun, 2005), and quite appropriate for a gene whose name is *SHORT INTERNODES*. Unexpectedly, however, overexpression of *SHI* in *Populus*, although not in *Arabidopsis*, increased the number of internodes (Fig. 9d). This also explains why there was only a very minor effect on total plant height. The observed phenotypic differences may be a consequence of the developmental differences between *Populus* and *Arabidopsis* shoots; in *Arabidopsis*, the shoot is an inflorescence that normally has a determinate growth pattern, whereas, in *Populus*, the shoot is a true vegetative structure that grows indeterminately. The SHI dwarfing effect has only been demonstrated to date by heterologous ectopic expression of one other annual plant, the ornamental Kalanchoe (Lutken *et al.*, 2010). However, despite the conservation of the growth-retarding effect, other phenotypes related to leaf color and flower phenology were not observed in Kalanchoe. Therefore, it is also possible that the observed phenotypic differences may be a result of incomplete conservation of gene function.

The most plausible explanation for the increased internode number seen in the *35S::SHI Populus* transgenics is increased cytokinin concentration. Cytokinin affects the organization and activity of the shoot apical meristem (SAM) (Werner *et al.*, 2003); therefore, the increased concentrations of the precursor of one of the most potent

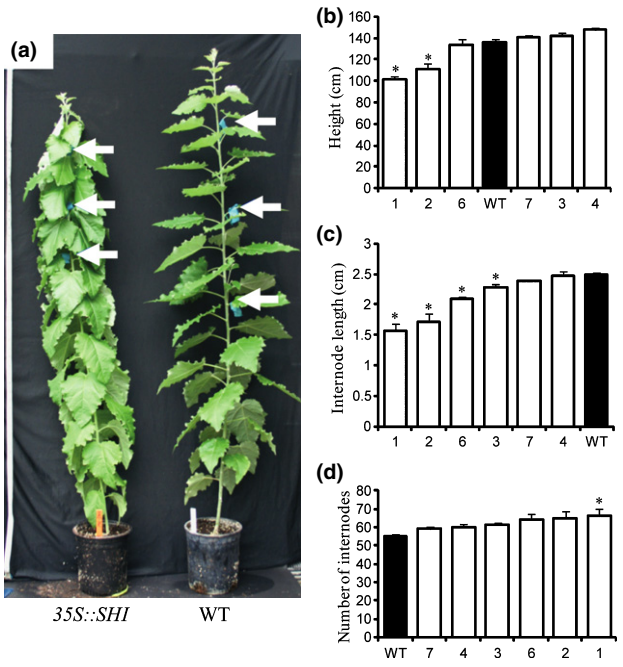

Fig. 9 Phenotypic changes in *35S::SHI Populus* transgenics. Measurements and photographs were obtained from 70-d-old, glasshouse-grown plants. (a) Arrows point to distances between 10 nodes of *35S::SHI* transgenic (left) and wild-type (WT) (right) plants. Bars represent event mean ± SE of seven ramets per transgenic event and 10 WT plants. Asterisks denote significant differences between transgenic and WT events as determined by ANOVA followed by Dunnett's *post-hoc* test ($P < 0.05$).

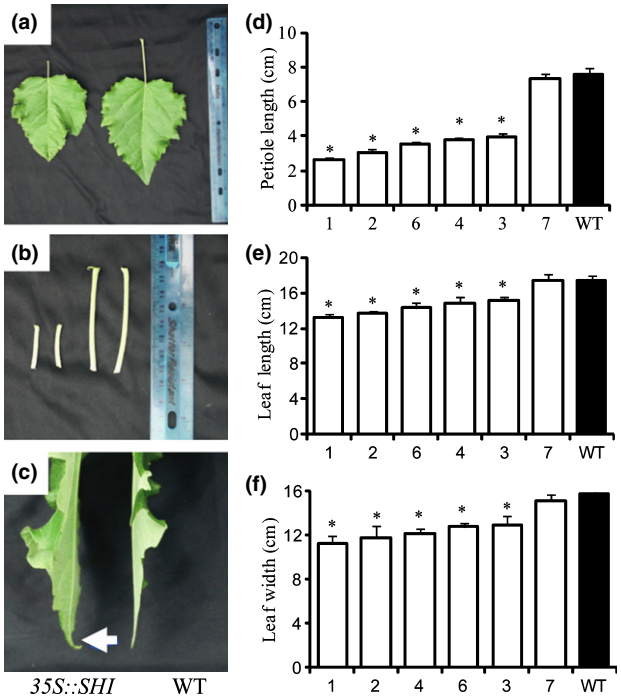

Fig. 10 Leaf morphology of *35S::SHI Populus* transgenics. Measurements (d–f) were performed on leaves from LPI30 (leaf plastochron index 30) of 70-d-old, glasshouse-grown plants. Photographs are representative of wild-type (WT; right) and transgenic (left) leaves (a), petioles (b) and leaf tips (c). In (c), the arrow points to a characteristic curl at the leaf apex in transgenics. Bars represent event mean ± SE for seven ramets per transgenic event and 10 WT plants. Asterisks denote significant differences between transgenic and WT events as determined by ANOVA followed by Dunnett's *post-hoc* test ($P < 0.05$).

cytokinins (IP), as observed, provides a logical explanation for the increased number of internodes. Unfortunately, cytokinin biosynthesis in plants is poorly understood. In the absence of a knowledge of the targets for putative *SHI* regulation, it was impossible to identify candidate genes that may be direct downstream targets. Alternatively, the effect of *SHI* overexpression on cytokinin concentration may be indirect. Nevertheless, the involvement of *SHI* or any other *SRS* genes in the regulation of cytokinin metabolism has not, to our knowledge, been reported previously; it clearly warrants further investigation.

Function of SHI in vegetative growth

The roles of SHI and its closely related family members STY1 and STY2 in reproductive development have been well characterized (Kuusk *et al.*, 2002, 2006; Sohlberg *et al.*, 2006). However, there is also evidence that these genes regulate vegetative development. For example, *SHI*, as well as *STY1* and *STY2*, has a dwarfing effect when overexpressed in *Arabidopsis* (Fridborg *et al.*, 1999; Kuusk *et al.*, 2002). Furthermore, overexpression and knock-outs of the three genes produce changes in leaf size, shape, curvature and serration (Kuusk *et al.*, 2002, 2006). The function of *SHI*-related genes in vegetative growth is also suggested by their expression in vegetative tissues. In this study, we showed that reduced expression of *PtaSHI1* and *PtaSHI2* promotes stem and leaf growth (Fig. 4). These effects are not surprising given the dwarfing effect caused by ectopic expression of *SHI* in *Arabidopsis*. However, increased vegetative growth from single or multiple loss-of-function mutations in *SHI* and its close relatives *STY1* and *STY2* has not been reported previously. One explanation is that these genes have undergone functional divergence. Alternatively, it is clear that *Populus* and *Arabidopsis* have very different growth habits and developmental trajectories, as discussed above with respect to the inflorescence vs. stem. Thus, the very short true vegetative phase of *Arabidopsis*, when compared with the extensive vegetative phase in *Populus*, may be the cause of the observed phenotypic differences.

STY1 and *STY2* genes have also been implicated in the control of vascular development of the gynoecium and, in particular, vascular patterning and proliferation of xylem tissue (Kuusk *et al.*, 2002). Defects of leaf venation in these mutants also suggest possible defects in xylem formation in vegetative tissues (Kuusk *et al.*, 2006). However, the roles of these genes in stem vasculature and/or wood formation have

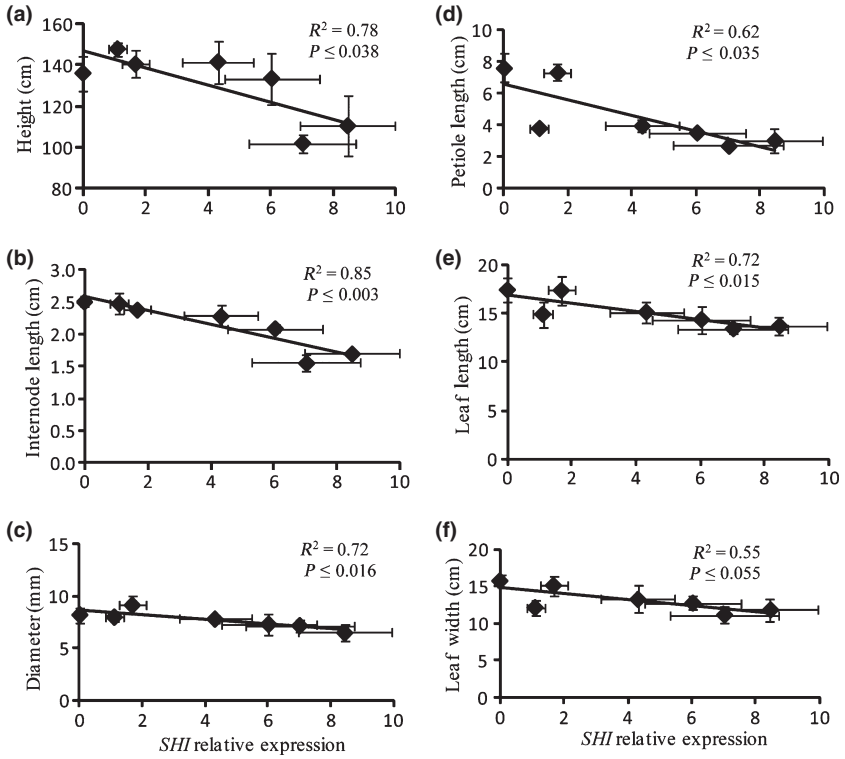

Fig. 11 Relationships between traits and transgene expression in *35S::SHI Populus* transgenics. Data points represent the event mean ± SE of seven ramets (based on expression results in Fig. 7 and trait measurements in Figs 9 and 10).

Table 3 Biomass analysis of transgenic plants

Event	Stem	Leaf	Petiole	Root
35S::SHI				
2	57 ± 8*	65 ± 13*	45 ± 7*	39 ± 2*
1	66 ± 7*	78 ± 6	50 ± 4*	48 ± 14*
3	96 ± 6	94 ± 2	68 ± 4*	77 ± 9*
7	106 ± 7	108 ± 9	116 ± 7	115 ± 25
Transgenic average	81 ± 7	86 ± 5	70 ± 7	70 ± 25
WT	100 ± 11	100 ± 5	100 ± 7	100 ± 6
RNAi				
1	175 ± 5*	141 ± 16*	125 ± 8*	188 ± 54*
12	178 ± 7*	140 ± 5*	140 ± 3*	185 ± 20*
Transgenic average	177 ± 2	141 ± 1	133 ± 11	187 ± 2
WT	100 ± 3	100 ± 30	100 ± 11	100 ± 10

Event mean ± SE for dry weight biomass relative to wild-type (WT) (%WT) in *35S::SHI* and *PtSHI1_2*-RNAi transgenic *Populus*.
*, $P \leq 0.05$.

Table 4 Hormone changes in transgenic plants

	Genotype		
	WT	*35S::SHI*	Fold change
GA_1	1.0647	7.53445	7.1
GA_{20}	13.6841	4.715	−2.9
GA_{53}	1.4082	0.4124	−3.4
GA_8	120.127	51.2919	−2.3
IPR	0.07173	0.4039	5.6
	WT	RNAi	
GA_4	2.2953	0.84659	−2.7
GA_9	33.4608	13.6142	−2.5
IP	0.09433	0.0405	−2.3

Concentrations of all hormones are shown in ng g^{-1} dry weight. Data represent the means of at least two independent events and biological replications. All changes were significant at least at $P < 0.05$ and determined using Student's *t*-test. GA, gibberellins; IP, N^6-isopentenyladenine; IPR, N^6-isopentenyladenosine.

not been described previously. We showed that the down-regulation of *PtaSHI1* and *PtaSHI2* increased secondary xylem (i.e. wood; Fig. 6) as a result of enhanced cell proliferation.

One explanation for the observed alterations in xylem development is a change in GA metabolism. GA has been implicated in the positive regulation of xylem cell proliferation (Wareing, 1958; Biemelt *et al.*, 2004; Israelsson *et al.*, 2005; Bjorklund *et al.*, 2007; Mauriat & Moritz, 2009), and *SHI* misexpression causes widespread changes in the GA-related metabolite pools (Fridborg *et al.*, 1999). Our GA measurements in the RNAi transgenics showed that the concentration of bioactive GA_1 was unchanged, whereas GA_4 was significantly down-regulated. Therefore, the observed increase in xylem fiber length cannot be explained by increased levels of bioactive GAs.

We believe that this study is the first report of GA concentration changes in any SRS loss-of-function genotype. In *Arabidopsis*, the overexpression of *SHI* leads to increased bioactive GA pools (Fridborg *et al.*, 1999). In this study,

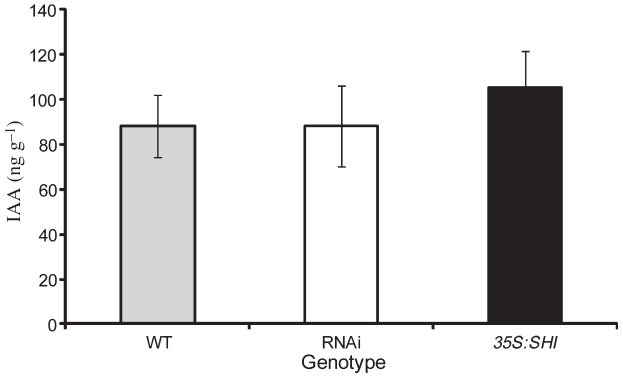

Fig. 12 Auxin (indole acetic acid, IAA) concentrations in transgenic plants. Bars show mean ± SE of two independent events and biological replications. None of the differences were significant as determined by Student's *t*-test at $P < 0.05$. WT, wild-type.

we showed that the down-regulation of two putative poplar SHI orthologs leads to the opposite effect – a decrease in at least one of the bioactive GAs (e.g. GA_4). Although these two reports come from different species, the fact that *SHI* up-regulation increases, whereas down-regulation decreases, bioactive GAs suggests the involvement of SHI in the regulation of GA metabolism and/or signaling.

The wood formation abnormalities observed could, at least in part, be related to changes in auxin concentrations. In *Arabidopsis*, *STY1* has been found to be a positive regulator of *YUCCA4*, a flavin monooxygenase involved in auxin biosynthesis (Sohlberg *et al.*, 2006; Eklund *et al.*, 2010). *YUCCA* genes interact with *STY1* and *STY2* to regulate floral vascular development (Sohlberg *et al.*, 2006). Moreover, a recent study has shown that STY1 and, possibly, other SHI/STY members are transcriptional activators of genes encoding proteins that mediate local auxin biosynthesis (Eklund *et al.*, 2010). Although our tissue level auxin measurements do not seem to indicate significant changes in RNAi transgenics, we cannot exclude the possibility that localized changes in auxin transport or sensitivity lead to the observed phenotypes.

Value for the manipulation of tree growth and form

The genes that control variation in the yield and form of tree crops are largely unknown (Busov *et al.*, 2008; Krizek, 2009). In this study, we present evidence for the first time that genes from the *Populus SRS* gene family may provide tools for the manipulation of stem and shoot growth, form and root morphology. The manipulation of endogenous *SHI* activity in *Populus*, using heterologous or native transgene forms, modified several aspects of plant growth, stature and form in an incremental manner that was correlated with gene expression levels. The overexpression of *Arabidopsis SHI* in *Populus* seems to provide very moderate inhibition of height growth, but severely reduces petiole growth, creating a highly compact plant form that may be well suited to high-density bioenergy plantings. Conversely, RNAi suppression of two *Populus SHI*-like genes had a growth-promoting effect on the leaves, stems and roots, and thus may benefit production in low-density stands where trees have ample space for rapid growth. The observed increase in stem girth could lead to an increase in harvest index for woody stems, and thus help to elevate biomass productivity. Because *SHI* genes act in a synergistic and redundant manner, it will be worthwhile to explore the effects of additional *SRS* gene family members independently and in combination. Because of the complex interactions of hormone- and growth-modifying genes with the environment, it is essential that translational studies move into the field.

Acknowledgements

This work was supported in part by grants from the US Department of Energy, Poplar Genome Based Research for Carbon Sequestration in Terrestrial Ecosystems (DE-FG02-06ER64185, DE-FG02-05ER64113), the Consortium for Plant Biotechnology Research, Inc. (GO12026-203A), the USDA CSREES, Biotechnology Risk Assessment Research Grants Program (2004-35300-14687), and grants from the National Natural Science Foundation of China (NSF 30630053) and China MOST '973' Project (G1999016005).

References

Biemelt S, Tschiersch H, Sonnewald U. 2004. Impact of altered gibberellin metabolism on biomass accumulation, lignin biosynthesis, and photosynthesis in transgenic tobacco plants. *Plant Physiology* **135**: 254–265.

Bjorklund S, Antti H, Uddestrand I, Moritz T, Sundberg B. 2007. Cross-talk between gibberellin and auxin in development of *Populus* wood: gibberellin stimulates polar auxin transport and has a common transcriptome with auxin. *Plant Journal* **52**: 499–511.

Braatne JH, Hinckley TM, Stettler RF. 1992. Influence of soil-water on the physiological and morphological components of plant water-balance in *Populus trichocarpa*, *Populus deltoides* and their F1 hybrids. *Tree Physiology* **11**: 325–339.

Busov V, Meilan R, Pearce DW, Rood SB, Ma C, Tschaplinski TJ, Strauss SH. 2006. Transgenic modification of *gai* or *rgl1* causes dwarfing and alters gibberellins, root growth, and metabolite profiles in *Populus*. *Planta* **224**: 288–299.

Busov VB, Brunner AM, Meilan R, Filichkin S, Ganio L, Gandhi S, Strauss SH. 2005. Genetic transformation: a powerful tool for dissection of adaptive traits in trees. *New Phytologist* **167**: 9–18.

Busov VB, Brunner AM, Strauss SH. 2008. Genes for control of plant stature and form. *New Phytologist* **177**: 589–607.

Busov VB, Meilan R, Pearce DW, Ma C, Rood SB, Strauss SH. 2003. Activation tagging of a dominant gibberellin catabolism gene (*GA 2-oxidase*) from poplar that regulates tree stature. *Plant Physiology* **132**: 1283–1291.

Chen WQ, Gai Y, Liu SC, Wang RX, Jiang XN. 2010. Quantitative analysis of cytokinins in plants by high performance liquid

chromatography: electronspray ionization ion trap mass spectrometry. *Journal of Integrative Plant Biology* **52**: 925–932.

Eklund DM, Staldal V, Valsecchi I, Cierlik I, Eriksson C, Hiratsu K, Ohme-Takagi M, Sundstrom JF, Thelander M, Ezcurra I *et al.* 2010. The *Arabidopsis thaliana* STYLISH1 protein acts as a transcriptional activator regulating auxin biosynthesis. *Plant Cell* **22**: 349–363.

Filichkin SA, Wu Q, Busov V, Meilan R, Lanz-Garcia C, Groover A, Goldfarb B, Ma CP, Dharmawardhana P, Brunner A *et al.* 2006. Enhancer trapping in woody plants: isolation of the ET304 gene encoding a putative AT-hook motif transcription factor and characterization of the expression patterns conferred by its promoter in transgenic *Populus* and Arabidopsis. *Plant Science* **171**: 206–216.

Fleet CM, Sun TP. 2005. A DELLAcate balance: the role of gibberellin in plant morphogenesis. *Current Opinion in Plant Biology* **8**: 77–85.

Franklin G. 1945. Preparation of thin sections of synthetic resins and wood–resin composites, and a new macerating method for wood. *Nature* **155**: 51.

Fridborg I, Kuusk S, Moritz T, Sundberg E. 1999. The *Arabidopsis* dwarf mutant *shi* exhibits reduced gibberellin responses conferred by overexpression of a new putative zinc finger protein. *Plant Cell* **11**: 1019–1031.

Fridborg I, Kuusk S, Robertson M, Sundberg E. 2001. The *Arabidopsis* protein SHI represses gibberellin responses in *Arabidopsis* and barley. *Plant Physiology* **127**: 937–948.

Gleave AP. 1992. A versatile binary vector system with a T-DNA organizational-structure conducive to efficient integration of cloned DNA into the plant genome. *Plant Molecular Biology* **20**: 1203–1207.

Gou J, Strauss SH, Tsai CJ, Fang K, Chen Y, Jiang X, Busov VB. 2010. Gibberellins regulate lateral root formation in *Populus* through interactions with auxin and other hormones. *Plant Cell* **22**: 623–639.

Graham RL. 1994. An analysis of the potential land base for energy crops in the Conterminous United States. *Biomass & Bioenergy* **6**: 175–189.

Holsters M, de Waele D, Depicker A, Messens E, van MM, Schell J. 1978. Transfection and transformation of *Agrobacterium tumefaciens*. *Molecular & General Genetics* **163**: 181–187.

Israelsson M, Sundberg B, Moritz T. 2005. Tissue-specific localization of gibberellins and expression of gibberellin-biosynthetic and signaling genes in wood-forming tissues in aspen. *Plant Journal* **44**: 494–504.

Jansson S, Douglas CJ. 2007. *Populus*: a model system for plant biology. *Annual Review of Plant Biology* **58**: 435–458.

Kim SG, Lee S, Kim YS, Yun DJ, Woo JC, Park CM. 2010. Activation tagging of an Arabidopsis SHI-RELATED SEQUENCE gene produces abnormal anther dehiscence and floral development. *Plant Molecular Biology* **74**: 337–351.

Krizek BA. 2009. Making bigger plants: key regulators of final organ size. *Current Opinion in Plant Biology* **12**: 17–22.

Kuusk S, Sohlberg JJ, Eklund DM, Sundberg E. 2006. Functionally redundant SHI family genes regulate Arabidopsis gynoecium development in a dose-dependent manner. *Plant Journal* **47**: 99–111.

Kuusk S, Sohlberg JJ, Long JA, Fridborg I, Sundberg E. 2002. STY1 and STY2 promote the formation of apical tissues during Arabidopsis gynoecium development. *Development* **129**: 4707–4717.

Livak KJ, Schmittgen TD. 2001. Analysis of relative gene expression data using real-time quantitative PCR and the 2(T)(–Delta Delta C) method. *Methods* **25**: 402–408.

Lutken H, Jensen LS, Topp SH, Mibus H, Muller R, Rasmussen SK. 2010. Production of compact plants by overexpression of AtSHI in the ornamental Kalanchoe. *Plant Biotechnology Journal* **8**: 211–222.

Mauriat M, Moritz T. 2009. Analyses of GA20ox- and GID1-over-expressing aspen suggest that gibberellins play two distinct roles in wood formation. *Plant Journal* **58**: 989–1003.

Sasaki A, Ashikari M, Ueguchi-Tanaka M, Itoh H, Nishimura A, Swapan D, Ishiyama K, Saito T, Kobayashi M, Khush GS *et al.* 2002. Green revolution: a mutant gibberellin-synthesis gene in rice. *Nature* **416**: 701–702.

Smith DL, Fedoroff NV. 1995. Lrp1, a gene expressed in lateral and adventitious root primordia of Arabidopsis. *Plant Cell* **7**: 735–745.

Sohlberg JJ, Myrenas M, Kuusk S, Lagercrantz U, Kowalczyk M, Sandberg G, Sundberg E. 2006. STY1 regulates auxin homeostasis and affects apical-basal patterning of the Arabidopsis gynoecium. *Plant Journal* **47**: 112–123.

Thomas SG, Sun TP. 2004. Update on gibberellin signaling. A tale of the tall and the short. *Plant Physiology* **135**: 668–676.

Wareing PF. 1958. Interaction between indole-acetic acid and gibberellic acid in cambial activity. *Nature* **181**: 1744–1745.

Werner T, Motyka V, Laucou V, Smets R, Van Onckelen H, Schmulling T. 2003. Cytokinin-deficient transgenic Arabidopsis plants show multiple developmental alterations indicating opposite functions of cytokinins in the regulation of shoot and root meristem activity. *Plant Cell* **15**: 2532–2550.

Wullschleger SD, Jansson S, Taylor G. 2002. Genomics and forest biology: *Populus* emerges as the perennial favorite. *Plant Cell* **14**: 2651–2655.

Yang XH, Kalluri UC, Jawdy S, Gunter LE, Yin TM, Tschaplinski TJ, Weston DJ, Ranjan P, Tuskan GA. 2008. The F-box gene family is expanded in herbaceous annual plants relative to woody perennial plants. *Plant Physiology* **148**: 1189–1200.

Supporting Information

Additional supporting information may be found in the online version of this article.

Table S1 Primers used in expression analyses

Please note: Wiley-Blackwell are not responsible for the content or functionality of any supporting information supplied by the authors. Any queries (other than missing material) should be directed to the *New Phytologist* Central Office.